# ENTANGLEMENT OF THERMAL STATE OF QUANTUM ANNEALING PROCESSOR

by

## Abdel-Haleem ABDEL-ATY[a,b*], Ahmad N. KHEDR[b], Amr A. YOUSSEF[c], and Yasser B. SADDEEK[b,d]

[a] Department of Physics, College of Sciences, University of Bisha, Bisha, Saudi Arabia
[b] Physics Department, Faculty of Science, Al-Azhar University, Assiut, Egypt
[c] Higher Institute for Engineering and Technology, El-Beheira, Egypt
[d] Physics Department, College of Science in Zulfi, Majmaah University, Al Majmaah, Saudi Arabia

*We investigate the dynamics of quantum correlations between the quantum annealing processor nodes. The quantum annealing processor is simulated by spin-chain model. It is assumed that system started from the thermal state. The Hamiltonian of the system is mathematically designed and analytically solved. The properties of the system are investigated. Negativity is used to investigate the dynamics of quantum correlation between the system nodes. The effect of the system parameters (spin-orbit coupling, coupling constant, and bias parameter) on the dynamics of negativity is explored. Results showed that the coupling constant had a great effect in the dynamics of the quantum correlation.*

Key words: *concurrence, thermal state, spin-orbit coupling, coupling constant, spin-chain model*

## Introduction

Spin-chain systems have attracted much interest with manufacturing the quantum computers. The recent version of quantum computers is designed based on the quantum annealing processor [1-6], which is one of the examples of spin-chains and gives a powerful results in fabrication of the quantum computers. On the other hand, the types of materials are classified as ferromagnetic or antiferromagnetic materials [7, 8] based on the type of the spin direction. Several experimental and theoretical studies extensively investigated the properties of spin-chain systems. The recent experiment by IBM reported 512 qubit quantum annealing processor, and used in solving very complex computer algorithms [9-14].

The quantum correlation is considered the key source of all applications in quantum information processing (computation, communications, metrology, and quantum computing) [15-17]. Recently, the quantum correlation between the photons has been generated to more than 2200 Km. Moreover this channel is used to transfer information between the correlated photons which are considered the basic work for the long range quantum communication (satellite communication) [18, 19]. Also, the correlation between the spins is the carrier of the data between them. Thus, generation of the correlation between the spin-chain is much required and

---

enable the spin-chain is a wire can transport the data across this wire. Bose proposed a protocol for information transfer over the spin-chain which is implemented experimentally. One of the best examples of the spin chains is the superconducting qubits. The quantum information is transferred between array of four superconducting qubits with the nearest-neighbor coupling with speed of 84 ns and high fidelity 99.2% in single step. This experiment represents the quantum wire transfer based on spin-chains, where with spin-chain, the data transfer with movement of the spins. The next step in the future is to realize devices to transfer the quantum data for a long distance through spin-chains. This adds a desirable tool for future applications in quantum information processing [20, 21]. In addition, flexibility of changing the values and different configurations of the coupling between the qubits plays an important role in quantum simulation of many-body systems, and studies its physical properties. As an example of the many body system, the quantum correlation between 2 and 8 qubits is investigated by Lanting *et al*. who, open the door for the real use of multi-qubits quantum annealing processor [22].

The dynamics of classical and quantum correlations over spin-chains [23, 24] and under some physical parameters (isoptopic and anistropic interactions, uniform and non-uniform magnetic fields and temperature) has been investigated in some Heisenberg spin-chain models. An examples of the spin-chain model is the Ising model [25, 26], XX and XY models [27, 28]. Moreover, spin-chain is modeled by another Heisenberg XXX model [29], XXZ [30], and XYZ model [31, 32]. In the XXX spin chain models, it is observed that the ferromagnetic $J < 0$ destroys the spin states entanglement, while the antiferromagnetic $J > 0$ generates much entanglement between the spins in the presence of temperature [33].The anisotropic antisymmetric exchange interaction which is presented by Moriya and Dzialoshinskii and mathematically expressed by $\vec{D}\,[\vec{S}_1 \times \vec{S}_2]$ has a great effect on the dynamics of the quantum and classical correlations between spins. The DM interaction was studied for several models of the spin-chain systems [34, 35]. In addition the effect of DM interaction and other parameters (spin-orbit coupling, Ising coupling, temperature and magnetic field) on the dynamics of classical and quantum correlations over spin-chain models is reported in [36-40]. The dynamics of classical and quantum correlations depends on the distance between spins, as well as other physical parameters in case realistic systems, such as short-range entanglement between spins or charge degrees of freedom, are observed in quantum dots, nanotube or molecules [41-43]. Most of the previous work considered the two-qubit systems, but Metwally and Abdel-Aty introduced some models of quantum networks consisting of multi-spins. Other studies addressed the effect of the magnetic fields and DM-interactions on the quantum properties of the system [44-47].

## Quantum annealing processor in thermal state

This section handles the discussion of the spin-chain model of the quantum annealing processor. To study the dynamics of the quantum correlation over the proposed model, several steps should be conducted, In this model, we proposed that the spins started from the thermal state. The theoretical model is mathematically designed by the spin-chain model. The unitary operator method is used for solving the system analytically. The impact of the system parameters will be clarified. The final density state of the system in the thermal state is obtained. The quantum correlation is quantified by the negativity measure.

### The Model and its solution

The quantum annealing model was introduced long times ago. DiCarlo *et al.* [4] introduced the first quantum processor manufactured based on the quantum annealing model. This work was followed by the paper of Lanting *et al.* [22], who successfully fabricated eight

Abdel-Aty, A.-H., *et al.*: Entanglement of Thermal State of Quantum Annealing ...
THERMAL SCIENCE: Year 2020, Vol. 24, Suppl. 1, pp. S325-S332

S327

quaits quantum annealing processor and invistigated the dynamics of the entanglement between the processor qubits. This was the first step towards fabricating multi-qubits quantum annealing processor for real use.

The following eq. (1) represents the two-qubit anisotropic Heisenberg XXZ model (spin chain model) of quantum annealing processor:

$$H = J_{zz}\sigma_{z_1} \otimes \sigma_{z_2} + \left(K_{x1}\sigma_{x_1} + K_{x2}\sigma_{x_2}\right) + \left(K_{z_1}\sigma_{z_1} + K_{z_2}\sigma_{z_2}\right) \tag{1}$$

where $\sigma_{\gamma m}(\gamma = x, y, z; m = 1, 2)$ is the Pauli matrices of the $n^{th}$ qubit, and $K_{\gamma m}$ – the coupling constant between two neighboring qubits, $J_{zz}$ – the real coupling constant for the spin interaction and the magnetic fields on the two qubits are:

$$\frac{B_{x,z}}{2}\left(1 - \delta_{x,z}\right), \text{ and } \frac{B_{x,z}}{2}\left(1 + \delta_{x,z}\right), \text{ respectively}$$

here

$$K_{x_1,z_1} = \frac{B_{x,z}}{2}\left(1 + \delta_{x,z}\right), \ K_{x_2,z_2} = \frac{B_{x,z}}{2}\left(1 - \delta_{x,z}\right)$$

where $B_{x,z}$ is external magnetic field of $x$- and $z$-axis, and – the parameter $\delta_{x,z}$ – the degree of inhomogenity with $0 \leq \delta_{x,z} \leq 1$, $K_{xm} > 0$, and $J_{zz} > 0$ correspond to the anti-ferromagnetic case, while $K_{xm} < 0$ and $J_{zz} < 0$ correspond to the ferromagnetic case. This model can be reduced to the isotropic XXX model and the isotropic XX model when $J_{zz} = K_{xm}$ and $J_{zz} = 0$, respectively. In the standard basis $\{|00>, |01>, |10>, |11>\}$, we express as the Hamiltonian (1) by matrix:

$$H = \begin{pmatrix} J_{zz} + A & K_{x_1} & K_{x_2} & 0 \\ K_{x_1} & -J_{zz} + B & 0 & K_{x_2} \\ K_{x_2} & 0 & -J_{zz} + C & K_{x1} \\ 0 & K_{x_2} & K_{x_1} & J_{zz} - A \end{pmatrix} \tag{2}$$

where $A = (K_{z_1} + K_{z_2})$, $B = (-K_{z_1} + K_{z_2})$, and $C = (K_{z_1} - K_{z_2})$.

*Evaluation of eigenvalues and corresponding eigenvectors*

In this part, we aim to find the eigenvalues and corresponding eigenvectors of this system, which will help us to find the final the density state of the system and consequently study all properties of the system.

First, the eigenvalues and eigenstates of the Hamiltonian can be obtained:

$$\mathbf{H}|\Psi_i\rangle = \mathbf{E}_i|\Psi_i\rangle \quad (i = 1, 2, 3, 4) \tag{3}$$

By implementing some calculations, the eigen-energy levels can be written:

$$E_{1,2} = J_{zz} \pm \varepsilon_1, \ E_{3,4} = -J_{zz} \pm \varepsilon_2, \ \varepsilon_1 = \sqrt{K_{x1}^2 + K_{x2}^2 + (K_{z1} + K_{z2})^2},$$
$$\varepsilon_2 = \sqrt{K_{x1}^2 + K_{x2}^2 + (K_{z1} - K_{z2})^2} \tag{4}$$

and the corresponding wave functions:

$$|\phi_j\rangle = A_{1j}|00\rangle + A_{2j}|10\rangle + A_{3j}|01\rangle + A_{4j}|11\rangle \tag{5}$$

where

$$\sum_1^4 |A_j|^2 = 1, \ j = 1, 2, 3, 4$$

$$
\begin{aligned}
|\phi_1\rangle &= A_{11}|00\rangle + A_{21}|10\rangle + A_{31}|01\rangle + A_{41}|11\rangle \\
|\phi_2\rangle &= A_{12}|00\rangle + A_{22}|10\rangle + A_{32}|01\rangle + A_{42}|11\rangle \\
|\phi_3\rangle &= A_{13}|00\rangle + A_{23}|10\rangle + A_{33}|01\rangle + A_{43}|11\rangle \\
|\phi_4\rangle &= A_{14}|00\rangle + A_{24}|10\rangle + A_{34}|01\rangle + A_{44}|11\rangle
\end{aligned}
\tag{6}
$$

*Evaluation the density state of the system*

Using the results in the previous Section *Evaluation of eigenvalues and corresponding eigenvectors*, it is easy to find the final density state of the system at thermal equilibrium from:

$$
\rho(T) = \frac{1}{Z} e^{-H/K_\beta T} = \frac{1}{Z} e^{-E_i/K_\beta T} |\phi_i\rangle\langle\phi_i|
\tag{7}
$$

where $E_i$ is the energy eigenvalues, $|\phi_i\rangle$ – the orthonormal bases, $\rho(T)$ – the density of thermal equilibrium, the state of a spin chain system and $Z = tr(e^{-H/K_\beta T})$ (is the partition function of the system) characterizes a partition function, $H$ – the system Hamiltonian, $K_\beta$ – the Boltzmann constant which equals 1, and $T$ – the temperature. Here, $\rho(T)$ symbolizes a thermal state, so the entanglement in the thermal state is called thermal entanglement (quantum collision). In the standard basis $\{|00\rangle, |01\rangle, |10\rangle, |11\rangle\}$ , the thermal density matrix $\rho(T)$ can be expressed:

$$
\rho(T) = \begin{pmatrix}
\rho_1 & \rho_5 & \rho_6 & \rho_7 \\
\rho_5^* & \rho_2 & \rho_8 & \rho_9 \\
\rho_6^* & \rho_8^* & \rho_3 & \rho_{10} \\
\rho_7^* & \rho_9^* & \rho_{10}^* & \rho_4
\end{pmatrix}
\tag{8}
$$

where the element matrix:

$$
\rho_m = \sum_{j=1}^{4} \frac{1}{Z} e^{-E_j/K_\beta T} A_{mj}^2, \quad m = 1, 2, 3, 4
\tag{9}
$$

$$
\begin{aligned}
\rho_5 &= \sum_{j=1}^{4} \frac{1}{Z} e^{-\beta E_j} A_{1j} A_{2j}, \quad \rho_6 = \sum_{j=1}^{4} \frac{1}{Z} e^{-\beta E_j} A_{1j} A_{3j} \\
\rho_7 &= \sum_{j=1}^{4} \frac{1}{Z} e^{-\beta E_j} A_{1j} A_{4j}, \quad \rho_8 = \sum_{j=1}^{4} \frac{1}{Z} e^{-\beta E_j} A_{2j} A_{3j} \\
\rho_9 &= \sum_{j=1}^{4} \frac{1}{Z} e^{-\beta E_j} A_{2j} A_{4j}, \quad \rho_{10} = \sum_{j=1}^{4} \frac{1}{Z} e^{-\beta E_j} A_{3j} A_{4j}
\end{aligned}
\tag{10}
$$

$$
Z = tr\left(e^{-H/K_\beta T}\right) = 2\left[e^{-\beta J_{zz}}\cosh(\beta\varepsilon_1) + e^{\beta J_{zz}}\cosh(\beta\varepsilon_2)\right], \quad \beta = \frac{1}{KT}
\tag{11}
$$

In the following computation, we will write the natural unit system (Boltzmann constant $K = 1$).

## Numerical results and discussion

Several measures have been introduced to quantify the amount of classical and quantum correlation in quantum systems. The Shannon-entropy is one of the early measures used to quantify classical correlations in both classical and quantum systems. Also, Von Neumann

Abdel-Aty, A.-H., *et al.*: Entanglement of Thermal State of Quantum Annealing ...
THERMAL SCIENCE: Year 2020, Vol. 24, Suppl. 1, pp. S325-S332

S329

entropy, negativity, concurrence, quantum discord, and, *etc.*, also measures used in quantifying the generated correlations in the quantum systems [48, 49].

In this section, the generated quantum correlation between quantum annealing processor nodes in thermal state is quantified using negativity. The Peres-Horodecki gauge [50] gives a qualitative way for sentence whether the state is entangled or not, that is *PPT* norm. The negativity, which is quantitative version of the criterion, was developed by Vidal and Werner [51]. In order to obtain thermal entanglement for Hamiltonian eq. (1), we use the concept of negativity. The negativity behavior is calculated in ground state. Figure 1 shows negativity as a function of the temperature, $T$, for different exchange strength coupling constant $J_{zz}$. Figure 1(a) represents the dynamics of the generated correlations and quantified by the negativity measure, as a function of temperature under the effect of the system parameters, spin-orbit coupling, coupling constant and bias parameter. In fig 1(a), we choose small values of the coupling constant and bias parameter where $K_{x_1,x_2} = K_{z_1,z_2} = (1.5, 1.5)$ with different values of the spin orbit coupling. In this figure, the solid line represent the negativity when $J_{zz} = 1$ dot-dashed curve for $J_{zz} = 5$, dotted curve with $J_{zz} = 10$, and the dashed curve with $J_{zz} = 20$. We can see from the figure with small values spin orbit coupling $J_{zz} = 1$, that the negativity started from the maximum value $N = 0.39$ continues time goes on, the negativity decreases and reaches the minimum value $N = 0.15$ at $KT = 4$, and continues with this value with temperature increases. Moreover, by increasing the value of the spin-orbit coupling $J_{zz} = 5$, the negativity started as same with the last curve; and with time goes on, the negativity decreases and reaches the minimum value $N = 0.15$ at $KT = 8$. Moreover, by increasing the value of the spin-orbit coupling $J_{zz} = 10, 20$, the negativity increases and reaches the minimum value more later than the previous cases.
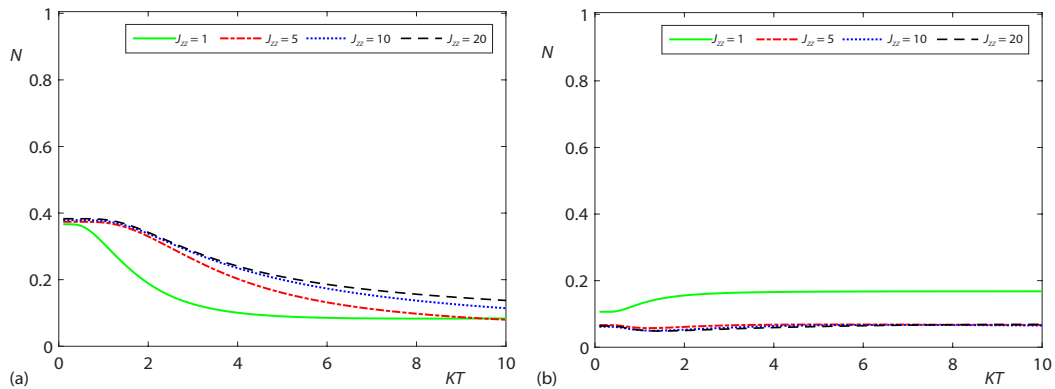


**Figure 1. The negativity as function of temperature $KT$, for different values of spin-orbit coupling $J_{zz}$;**
**(a) $K_{x_1,x_2} = K_{z_1,z_2} = (1.5, 1.5)$ and (b) $K_{x_1,x_2} = (1.5, 1.5)$, $K_{z_1,z_2} = (0.5, 0.5)$, and $J_{zz} = 1, 5, 10, 20$ for solid,**
**dash-dotted, dotted and dashed curves, respectively**

Figure 1(b) is the same as fig 1(a), but with small values of the bias parameter where $K_{x_1,x_2} = (1.5, 1.5)$ and $K_{z_1,z_2} = (0.5, 0.5)$. We can see in this figure that decreasing the value of the bias parameter led to the opposite effect compared to the previous figure. We can see that with small value of the spin-orbit coupling $J_{zz} = 5$, the negativity started from $N = 0.1$, increased with time increases and reached maximum value $N = 0.2$ at $KT = 2$. Over time, the negativity continues as a straight line. The effect of increasing the values of the spin-orbit coupling $J_{zz} = 5, 10, 20$ is depicted by the dotted, dash-dotted and dashed curves. We can see from these curves that increasing the value of the spin-orbit coupling and decreasing the values of bias parameter resulted in a decrease in the negativity even with increasing the temperature.

S330

Abdel-Aty, A.-H., *et al.*: Entanglement of Thermal State of Quantum Annealing ...
THERMAL SCIENCE: Year 2020, Vol. 24, Suppl. 1, pp. S325-S332

Figure 2 is the same as fig. 1 but with large values of the coupling constant and bias parameter. In fig. 2(a), the values of the coupling constants and bias parameter are $K_{x_1,x_2} = (5, 5)$, and $K_{z_1,z_2} = (1.5, 1.5)$. It shows the main contribution in the dynamics of the negativity results from the coupling constant and bias parameter, and the spin-orbit coupling has no effect. Furthermore, the negativity started from the maximum value $N = 0.4$, continues with the same value for all cases until $KT = 5$, and decreases again with temperature goes on. Here, we can say that the effect of the spin orbit coupling appears after $KT = 5$. Figure 2(b) is the same with fig. 2(a), but increasing the value of bias parameter $K_{z_1,z_2} = (0.5, 0.5)$. We can see the small difference between this figure and fig. 2(a), especially with large values of the temperature $KT$.
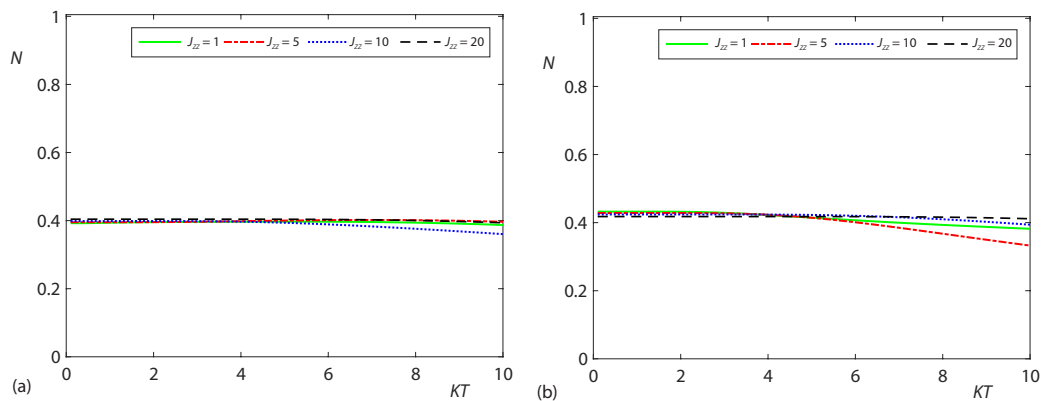


(a)  (b)

**Figure 2. The negativity as function of temperature $KT$, for different values of spin-orbit coupling $J_{zz}$; (a) $K_{x_1,x_2} = (5, 5)$, $K_{z_1,z_2} = (1.5, 1.5)$ and (b) $K_{x_1,x_2} = K_{z_1,z_2} = (5, 5)$, and $J_{zz} = 1, 5, 10, 20$ for solid, dash-dotted, dotted and dashed curves, respectively**
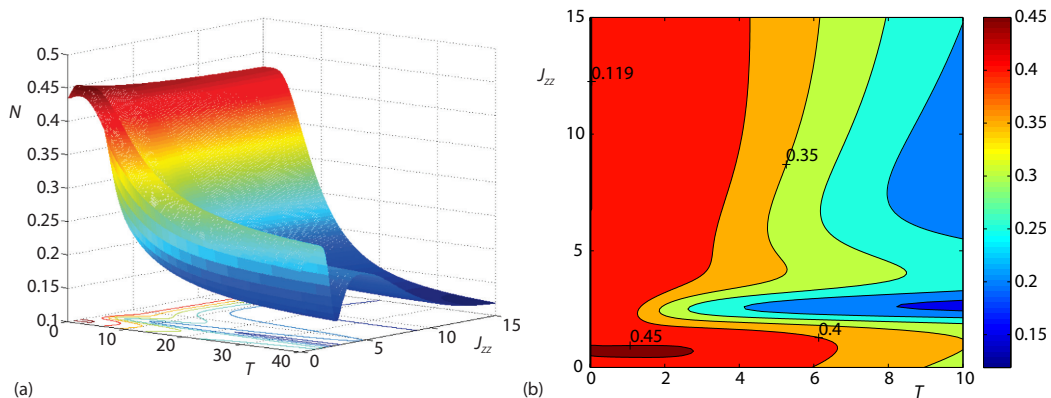


(a)  (b)

**Figure 3. Plot 3-D and contour of the dynamics of the negativity over quantum annealing processor, as function of $KT$ and spin-orbit coupling $J_{zz}$, with $K_{x_1,x_2} = (1.5, 1.5)$, $K_{z_1,z_2} = (1.5, 1.5)$**

In fig. 3, 3-D plot shows the effect of the spin orbit coupling on the dynamics of the quantum correlation as a function of the temperature over quantum annealing processor. It indicates that for the small value of the temperature, the spin-orbit coupling has no effect. By increasing the values of the spin-orbit coupling the negativity decreases. In addition, with increasing the spin-orbit coupling the negativity decreases and increasing again at $J_{zz} = 5$.

Abdel-Aty, A.-H., *et al.*: Entanglement of Thermal State of Quantum Annealing ...
THERMAL SCIENCE: Year 2020, Vol. 24, Suppl. 1, pp. S325-S332

S331

## Conclusion

The present paper addressed the dynamics of quantum correlation between the two-qubit quantum annealing processor nodes. It was proposed that the processor started from thermal state. The quantum correlation was quantified by the negativity. The dynamics of the quantum correlations under the effect of the model parameters was investigated. The results indicated that the system parameters played an important role in the dynamics of quantum correlations. We obtained maximum entanglement at some specific values of the system parameters. The maximum quantum correlation was obtained with large values of coupling constant and bias parameter as well as small values of the spin-orbit coupling.

## References

[1] Johnson, M., *et al*., Quantum Annealing with Manufactured Spins, *Nature*, *473* (2011), May, pp. 194-198
[2] Li, R. Y., *et al*., Quantum Annealing *vs*. Classical Machine Learning Applied to a Simplified Computational Biology Problem, *NPJ Quantum Inf*., *4* (2018), 14
[3] Vinci, W., *et al*., Nested Quantum Annealing Correction, *NPJ Quantum Inf.*, *2* (2016), 16017
[4] DiCarlo, L., *et al*., Demonstration of Two-Qubit Algorithms with a Superconducting Quantum Processor, *Nature*, *460* (2009), June, pp. 240-244
[5] Abdel-Aty, A.-H., *et al*., Thermal Entanglement in Quantum Annealing Processor, *International Journal of Quantum Information*, *16* (2018), 1850006
[6] Owyed, S., *et al*., Mathematical Modelling and Simulation of 3-Qubits Quantum Annealing Processor, *Proceedings*, 2nd International Conference on Mathematics and Statistics (ICoMS'19), Association for Computing Machinery, New York, USA, 2019, pp. 14-18
[7] Fukuhara, T., *et al*., Microscopic Observation of Magnon-Bound States and Their Dynamics, *Nature*, *502* (2013), Sept., pp. 76-79
[8] Furukawa, S., *et al*., Chiral Order and Electromagnetic Dynamics in 1-D Multiferroic Cuprates, *Phys. Rev. Lett*., *105* (2010), 257205
[9] Bunyk, P. I., *et al*., Architectural Considerations in the Design of a Superconducting Quantum Annealing Processor, *IEEE Transactions on Applied Superconductivity*, *24* (2014), 4, 1700110
[10] Boyda, E., *et al*., Deploying a Quantum Annealing Processor to Detect Tree Cover in Aerial Imagery of California, *PLoS ONE*, *12* (2017), e0172505
[11] Boixo, S., *et al*., Evidence for Quantum Annealing with More than one Hundred Qubits, *Nature Phys*, 10, (2014), Feb., pp. 218-224
[12] Mishra, A., *et al*., Performance of Two Different Quantum Annealing Correction Codes, *Quantum Inf Process*, *15* (2016), 2, pp. 609-636
[13] Homid, A. H., *et al*., Efficient Realization of Quantum Search Algorithm Using Quantum Annealing Processor with Dissipation, *Journal Opt. Soc. Am. B*, *32* (2015), 9, pp. 2025-2033
[14] Zidan, M., *et al*., Low-Cost Autonomous Perceptron Neural Network Inspired by Quantum Computation, *AIP Conference Proceedings*, *1905* (2017), 020005
[15] Michler, P., *et al*., Quantum Correlation among Photons from a Single Quantum Dot at Room Temperature, *Nature*, *406* (2000), Aug., pp. 968-970
[16] Inoue, S., *et al*., Quantum Correlation between Longitudinal-Mode Intensities in a Multimode Squeezed Semiconductor Laser, *Phys. Rev. A*, *46* (1992), 2757
[17] Ge, R., *et al*., Quantum Correlation and Classical Correlation Dynamics in the Spin-Boson Model, *Phys. Rev. A*, *81* (2010), 064103
[18] Yin, J., *et al*., Satellite-Based Entanglement Distribution over 1200 kilometers, *Science*, *356* (2017), 6343, pp. 1140-1144
[19] Yin, J., *et al*., Satellite-to-Ground Entanglement-Based Quantum Key Distribution, *Phys. Rev. Lett*., *119* (2017), 200501
[20] Li, X., *et al*., Perfect Quantum State Transfer in a Superconducting Qubit Chain with Parametrically Tunable Couplings, *Phys. Rev. Applied*, *10* (2018), 054009
[21] Kumar, S., *et al*., Towards Long-Distance Quantum Networks with Superconducting Processors and Optical Links, *Quantum Sci. Technol*., *4* (2019), 045003

[22] Lanting, T., *et al*., Entang in a Quantum Annealing Processor, *Phys. Rev*., *X4* (2014), May, 021 041

[23] Wootters, W. K., Entanglement of Formation of an Arbitrary State of Two Qubits, *Phys. Rev. Lerr*., *80* (1988), Mar., 2245

[24] Abdalla, M.-S., et al., Degree of Entanglement for Anisotropic Coupled Oscillators Interacting with a Single Atom, *Journale Opt. B: Quantum Semiclass. Op*t., *4* (2002), Oct., 396

[25] Gunlycke, D., *et al.*, Thermal Concurrence Mixing in a One-Dimensional Ising Model, *Phys. Rev. A*, *64* (2001), Sept, 0432302

[26] Childs, A. M., Asymptotic Entanglement Capacity of the Ising and Anisotropic Heisenberg Interactions, *Quantum Inf. Comput*., *3* (2003), 97

[27] Wang, X., Thermal and Ground-State Entanglement in Heisenberg XX Qubit Rings, *Phys. Rev. A*, *66* (2002), 034302

[28] Wang, X., Entanglement in the Quantum Heisenberg XY Model, *Phys. Rev. A*, *64* (2001), 012313

[29] Arnesen, M. C., *et al*., Natural Thermal and Magnetic Entanglement in the 1-D Heisenberg Model, *Phys. Rew. Lett*., *87* (2001), 017901

[30] Li, D.-C., *et al*., Thermal Entanglement in the Anisotropic Heisenberg XXZ Model with the Dzyaloshinskii-Moriya Interaction, *Journal Phys.: Condens. Matter*, *20* (2008), 325229

[31] Xi, X., Pairwise Thermal Entanglement in the n-Qubit Heisenberg XX Chain, *Phys. Lett. A*, *300* (2002), 567

[32] Rigolin, G.,Thermal Entanglement in the Two-Qubit Heisenberg XY Z Model, *Int. J. Quant. Inf*., *2* (2004) 393

[33] Hu, Z.-N., *et al*., Thermal Entanglement of a Three-Qubit System in Homogeneous Magnetic Fields, *Journal Phys. A: Math. Theor*., *40* (2007), 26, 7283

[34] Dzialoshinski, I., A Thermodynamic Theory of Weak Ferromagnetics, Journal Phys. Chem. Solida, 4, (1958), 4, pp. 241-255

[35] Moriya, T., Anistropic Superexchange Interaction and Weak Ferromagnetism, *Phys. Rev. Lett*., *120* (1960) 91

[36] Zhang, G. F., Li, S. S., Thermal Entanglement in a Two-Qubit Heisenberg XXZ Spin Chain under an Inhomogeneous Magnetic Field, *Phys. Rev. A*, *72* (2005), 034302

[37] Gu, S. J., *et al*., Universal Behaviors of Mutual Information in 1-D Model, *Phys. Rev. A*, *68* (2003), 042330

[38] Albayrak, E., Thermal Entanglement in the Anisotropic Heisenberg Model with Dzyaloshinskii-Moriya Interaction in an Inhomogeneous Magnetic Field, *Eur. Phys. B*, *72* (2009), 491

[39] Ercolessi, E., *et al*. Exact Entanglement Entropy of the XYZ Model and Its Sine-Gordon Limit, *Phys. Lett. A*, *374* (2010), 2101

[40] Zhou, L., *et al*., Enhanced Thermal Entanglement in an Anisotropic Heisenberg XYZ Chain, *Phys. Rev. A*, *68* (2003), 024301

[41] Redwan, A., *et al*., Dynamics of Classical and Quantum Information on Spin-chains with Multiple Interactions, *Inf. Sci. Lett*., *7* (2018), 2, pp. 29-33

[42] Redwan, A., *et al*., Dynamics of the Entanglement and Teleportation of Thermal State of a Spin Chain with Multiple Interactions, *Chaos*, *29* (2019), 013138

[43] Salah, R., *et al*., Pancharatnam Phase of Two Two-Level Atoms Interacting with a Time-Dependent Cavity Field, *Inf. Sci. Lett*., *8* (2019), 2, pp. 41-50

[44] Abdel-Aty, A.-H., *et al*., Effect of the Spin-Orbit Interaction on Partial Entangled Quantum Network, *Lecture Notes in Electrical Engineering*, *285* (2014), 529

[45] Abdel-Aty, A.-H., *et al*., Quantum Network Via Partial Entangled State, *Journal of Communications*, *9* (2014), 379

[46] Abdel-Aty, A., *et al*., Characteristics and Distinctive Features of Entanglement in Superconducting Charge Gubits, in: *Quantum Entanglement*, Nova Science Publishers Inc., New York, USA, 2012, pp. 199-243

[47] Abdel-Aty, A.-H., *et al*., Entanglement and Teleportation Via Partial Entangled-State Quantum Network, *Journal of Computational and Theoretical Nanoscience*, *12* (2015), 2213

[48] Shannon, C. E., A Mathematical Theory of Communication, *Bell System Technical Journal*, *27* (1984), July, pp. 379-423

[49] Eisert, J., Entanglement in Quantum Information Theory, Ph. D. thesis, University of Potsdam, Brandenburg, Germany, 2001

[50] Simon, R., Peres-Horodecki Separability Criterion for Continuous Variable Systems, *Physical Review Letters*, *84* (2000), Mar. 2726-2729

[51] Vidal, G., Werner, R. F., Computable Measure of Entanglement, *Phys. Rev. A*, *65* (2002), 032314